Engineering Fracture Mechanics 131 (2014) 687–701

Contents lists available at ScienceDirect

Engineering Fracture Mechanics

journal homepage: www.elsevier.com/locate/engfracmech

A fracture mechanics-based method for prediction of cracking of circular and elliptical concrete rings under restrained shrinkage

Wei Dong [a], Xiangming Zhou [b,*], Zhimin Wu [a]

[a] State Key Laboratory of Coastal and Offshore Engineering, Dalian University of Technology, Dalian 116024, PR China
[b] School of Engineering and Design, Brunel University, London UB8 3PH, UK

ARTICLE INFO

Article history:
Received 23 March 2014
Received in revised form 10 July 2014
Accepted 8 October 2014
Available online 16 October 2014

Keywords:
Brittle fracture
Concrete
Crack initiation
Environmental cracking
R-curves
Residual stresses
Stress intensity factor
Test standards

ABSTRACT

A new experimental method, utilizing elliptical ring specimens, is developed for assessing the likelihood of cracking and cracking age of concrete subject to restrained shrinkage. To investigate the mechanism of this new ring test, a fracture mechanics-based numerical approach is proposed to predict crack initiation in restrained concrete rings by using the *R*-curve method. It has been found that numerical results accord well with experimental results in terms of cracking ages for both circular and elliptical concrete rings, indicating that the proposed fracture mechanics-based numerical approach is reliable for analyzing cracking in concrete ring specimens subject to restrained shrinkage.

1. Introduction

When volume change of concrete from autogenous, drying or thermal shrinkage is restrained, residual stress will be developed and crack may occur once the residual tensile stress exceeds the tensile strength of concrete. This shrinkage cracking is a major problem for flat concrete elements/structures with a large exposed surface area-to volume (A/V) ratio, such as industrial floors, concrete pavements and bridge decks, in particular when concrete is at early ages. Cracking in concrete can reduce load carrying capacity and accelerate deterioration, which shortens the service life of concrete structures and increases maintenance costs. Therefore, researchers are seeking to develop simple tests to assess how susceptible a concrete mixture may be to cracking in decades. So far, such as the bar [1,2], the plate/slab [3,4] and the ring tests [5,6] have been developed to evaluate the cracking tendency of concrete under restrained conditions. However, it has been found difficulties in providing sufficient restraint in the bar and plate/slab tests [7]. On the other hand, the circular ring test has been widely used for assessing cracking tendency of concrete and other cement-based materials [8,9] due to its simplicity and versatility. It has subsequently become a standard test method for assessing cracking potential of concrete and other cement-based materials recommended by American Association of State Highway and Transport Officials (AASHTO) (i.e., AASHTO PP34-99: *Standard Practice for Cracking Tendency using a Ring Specimen*) and by American Society for Testing and Materials (ASTM)

* Corresponding author.
E-mail addresses: dongwei@dlut.edu.cn (W. Dong), Xiangming.Zhou@brunel.ac.uk (X. Zhou), wuzhimin@dlut.edu.cn (Z. Wu).

http://dx.doi.org/10.1016/j.engfracmech.2014.10.015
0013-7944/

Nomenclature

R	critical energy release rate (fracture resistance)
G	crack driving energy rate
R_0	internal radius of a circular concrete ring
R_i	external radius of a circular concrete ring
R_1	inner major radius of an elliptical concrete ring
R_2	inner minor radius of an elliptical concrete ring
d	wall thickness of a restraining steel ring
E	elastic modulus
f_t	splitting tensile strength
f_c	uniaxial compressive strength
t	age of concrete
K_{IC}	critical stress intensity factor
$CTOD_C$	critical crack tip opening displacement
a	crack length
a_c^f	critical crack length
w	concrete ring wall thickness
σ	nominal stress
T	fictitious temperature drop
α_c	linear expansion coefficient of concrete
a_c	critical crack length
a_0	initial crack length
α, β	coefficients of R-curve
$\varepsilon_{c\sigma}(t,t_0)$	stress–dependent strain at time t
$\sigma_c(t_0)$	stress in concrete at the time of loading t_0
$E_{ci}(t_0)$	elastic modulus of concrete at the time of loading t_0
$J(t,t_0)$	creep function
$\varphi(t,t_0)$	creep coefficient
$\Delta\sigma_\theta$	increment of the circumferential tensile stress

(i.e., ASTM C1581/C1581M-09a: *Standard Test Method for Determining Age at Cracking and Induced Tensile Stress Characteristics of Mortar and Concrete under Restrained Shrinkage*).

As a test method for assessing cracking potential of concrete, the ability of generating a visible crack within a short period is desirable for large amount of assessment of cracking tendency of concretes or other cement-based materials. However, it has been found that it may result in a fairly long period before the first cracking occurs in a restrained circular concrete ring due to either the restraining steel core is not stiff enough or the concrete is characterized with high crack resistance [10,11]. Besides, initial cracking may appear anywhere along the circumference of a circular ring specimen, making it difficult to be detected or traced in experiment. Therefore, although standard dimensions of circular ring specimens are recommended by AASHTO and ASTM, respectively, many researchers have used circular ring specimens with other geometries [8,9,11–15]. Meanwhile, a novel elliptical ring geometry was adopted for assessing cracking tendency of mortar under restrained condition. In this initiative, the first cracking was expected to occur earlier than in a circular geometry to shorten experiment duration. It was believed that there is higher stress intensity in an elliptical ring due to geometrical effect [16,17]. This initiative has been recognized as an effort to increase the stress concentration provided by the ring by Moon and Weiss [14]. It should be noted that, although it is generally regarded that higher degree of restraint can be provided by an elliptical geometry than a circular one in the restrained ring test, there is no evidence having been presented in scientific literature to validate this. So far, the researches related to elliptical concrete ring test [16–18] are focused on using elliptical ring test as a better tool than the circular ring test for estimating the cracking tendency of concrete or other cement-based materials. No much effort has been made on exploring the mechanism of the elliptical ring test or validating the advantages of elliptical geometry overwhelming circular geometry in shortening ring test which is still not clear to concrete science and engineering community.

A few theoretical/numerical models have been proposed to predict residual stress development and cracking age of concrete in restrained circular ring specimens. In a circular ring specimen, restraining effect from the central steel ring to the surrounding concrete ring is uniform along its circumference. Consequently, uniform circumferential tensile stress is resulted in the concrete ring along its circumference. Therefore, the restraining effect from the central steel ring on surrounding concrete can be conveniently replaced by a fictitious uniform pressure applied on the internal surface of the concrete ring in analytical/numerical analyses [11,12,19,20]. But, things are different in case of an elliptical geometry. The elliptical geometry produces a complicated and non-uniform circumferential stress in the elliptical concrete ring. Consequently, a closed-form analytical solution is not available for predicting residual stress development in an elliptical concrete ring subject to restrained shrinkage. Recently, Zhou et al. [21] conducted comparison test of a series of circular and elliptical concrete

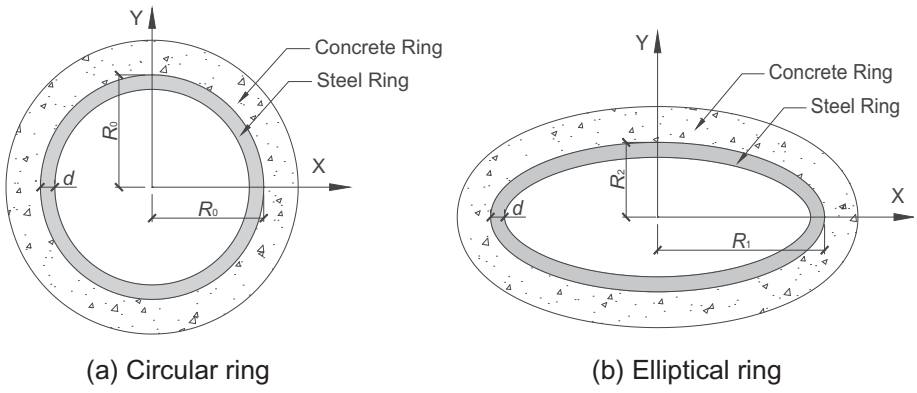

Fig. 1. Notation of geometrical parameters of circular and elliptical ring specimens.

rings and demonstrated the advantages of using elliptical rings over circular ones in faster and more reliable assessment of cracking potential of concrete. They also proposed an elastic damage model based on maximum tensile stress cracking criterion for predicting crack initiation in circular and elliptical concrete rings under restrained shrinkage.

On the other hand, cracking criteria for concrete, which is generally regarded as a quasi-brittle material, can be a controversial issue in concrete science and engineering community. Although cracking of concrete can be determined based on the conventional maximum tensile stress cracking criterion, some researchers [8,15,23] have criticized that such a tensile stress-based failure criterion might not yield accurate results for cracking of concrete at early ages, and a fracture-based cracking criterion tends to be more appropriate. In this case, the fracture resistance curve approach, which is based on fracture mechanics theory but is executed in the format of energy balance, has been widely used by many researches in analyzing cracking of concrete [8,15,19,22]. By comparing critical energy release rate (R-curve) and crack driving energy rate (G-curve), steady and unsteady crack propagation stages in concrete, as well as the critical moment of crack propagation evolving from steady to unsteady stage, can be determined. It should be noted that, the G-curve is closely related to the stress field around a crack in concrete and the shape and geometry of a concrete element. In the case of a restrained circular ring, the stress in concrete can be conveniently calculated by using the fictitious uniform pressure to simulate the effect of shrinkage in concrete. Stress intensity factor can also be approximately obtained by using a weighting function approach [23], in which R_0/R_i (R_0 and R_i are internal and external radius of a circular concrete ring, respectively) was introduced as a sole characteristic parameter for determining the coefficients of the geometry function. However, the R-curve approach based on fracture mechanics cannot be directly employed for analyzing cracking in an elliptical concrete ring. Firstly, as aforementioned, the assumption of a uniform pressure between a concrete and a steel ring is not appropriate for simulating the effect of shrinkage in an elliptical concrete ring due to the influence of its elliptical geometry. Secondly, compared with circular rings which are geometrically similar with geometry function depending on R_0/R_i only, elliptical rings are much complicated. Their geometry function not only depends on their inner major radius-to-outer major radius ratio, i.e. $R_1/(R_1 + d)$ with R_1 and d (d is the thickness of a steel ring) denoted in Fig. 1, but also the inner minor radius-to-outer minor radius ratio, i.e., $R_2/(R_2 + d)$ with R_2 denoted in Fig. 1, as well as the absolute values of the inner/outer major radiuses, i.e. $R_1 + d$ and $R_2 + d$, and the inner/outer minor radiuses, i.e. R_1 and R_2. So far, there is neither geometry function of stress intensity factor having been proposed for an elliptical ring, nor is the R-curve approach having been used to analyses cracking in a restrained elliptical concrete ring.

In line with these, a numerical approach was developed in this study to analyze fracture of concrete in restrained ring specimens subject to drying from their outer circumferential cylindrical surface. A fictitious temperature field, which is derived based on free shrinkage test of concrete prisms, was applied on concrete ring specimens in numerical analyses to simulate the mechanical effect of concrete shrinkage on rings under exposed condition. Secondly, a fracture-based failure criterion is employed to determine crack occurrence in concrete rings subject to restrained shrinkage. It is found that cracking ages of both circular and elliptical rings, predicted by the proposed numerical approach, agree reasonably well with experimental results, suggesting that the fracture-mechanics based numerical model, established in this research, is reliable for analyzing cracking in restrained concrete ring specimens. It is expected that the fracture mechanics-based numerical model developed in this study will be helpful in exploring the mechanism of restrained elliptical concrete ring test which can be employed for assessing cracking tendency of concrete and other cement-based materials.

2. Experimental program

The mix proportions for the concrete used for this study was 1:1.5:1.5:0.5 (cement:sand:coarse aggregate:water) by weight with the maximum aggregate size of 10 mm. Concrete was prepared using a drum-type mixer and various concrete specimens were made including 100 mm-diameter and 200 mm-length cylinders for measuring mechanical properties of

concrete, 75 mm in square and 280 mm in length prisms for free shrinkage test, notched beams with the dimensions of $100 \times 100 \times 500\ mm^3$ for fracture test and a series of circular and elliptical ring specimens for restrained shrinkage test. Ready-mixed concrete was poured into relevant concrete moulds in layers and vibrated thoroughly after each layer of concrete placement. Then the concrete specimens were covered by a layer of plastic sheet and cured in the normal laboratory environment for 24 h. Subsequently, all specimens were de-moulded and moved into an environment chamber with 23 °C and 50% relative humidity (RH) for continuous curing/drying. Mechanical properties of concrete, including elastic modulus E, splitting tensile strength f_t and uniaxial compressive strength f_c, were measured from the cylindrical specimens at 1, 3, 7, 14 and 28 days, three specimens tested for each mechanical property at each age.

2.1. Material properties

It has been found that the average 28-day compressive and splitting tensile strength of the concrete are 27.21 and 2.96 MPa, respectively, indicating that a normal strength concrete was prepared for this study. As aforementioned, only mechanical properties of concrete at the ages of 1, 3, 7, 14 and 28 days were physically measured. Based on experimental results, regression analyses were conducted to obtain continuous equations that can estimate the age-dependent mechanical properties, in this case, E and f_t, for the concrete. It was found that elastic modulus, E, in GPa of the concrete at early ages can be predicted using Eq. (1).

$$E(t) = 0.0002t^3 - 0.0134t^2 + 0.3693t + 12.715 \quad (t \leqslant 28) \tag{1}$$

Splitting tensile strength, f_t, in MPa can be predicted using Eq. (2).

$$f_t(t) = 1.82t^{0.13} \quad (t \leqslant 28) \tag{2}$$

In both equations, t is the age (unit: day) of concrete. The values of E and f_t for concrete at other ages which were not directly measured can be obtained from Eqs. (1) and (2).

In this study, fracture properties, including the critical stress intensity factor K_{IC} and the critical crack tip opening displacement $CTOD_C$, of concrete were derived based on the two-parameter fracture model (TPFM) recommended by RILEM [24] from experimental results of three-point bending tests of centrally notched beams, with the dimensions of $100 \times 100 \times 500\ mm^3$, the pre-crack length of 33.3 mm, and test span of 400 mm. All fracture tests were carried out under crack mouth opening displacement (*CMOD*) control model using an Instron 2670 series crack opening displacement gauge with a *CMOD* rate of 0.0075 mm/min. K_{IC} and $CTOD_C$, at the ages of 1, 3, 7, 14 and 28 days, were calculated conforming to RILEM recommendation in this study. Based on the experimental results of K_{IC} and $CTOD_C$ at the ages of 1, 3, 7, 14 and 28 days, regression analyses were conducted to obtain continuous equations for K_{IC} and $CTOD_C$, respectively. It is found that the K_{IC} in MPa $mm^{1/2}$ and $CTOD_C$ in mm of the concrete at early ages can be predicted as following:

$$K_{IC}(t) = 3.92\ln(t) + 12.6 \tag{3}$$

$$CTOD_C = -0.029t^2 + 1.62t + 3.96 \tag{4}$$

In the above two equations, t is the age (unit: day) of concrete.

2.2. Free shrinkage tests

Free shrinkage of concrete was measured on concrete prisms with the dimensions of 280 mm in length and 75 mm square in cross section, conforming to ISO 1920-8, subject to drying in the same environment condition as for curing concrete

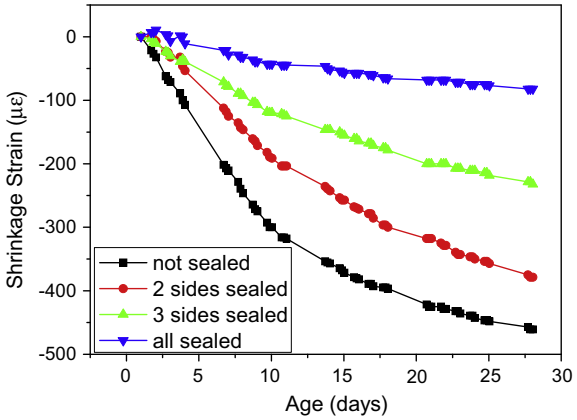

Fig. 2. Shrinkage strain of concrete obtained from free shrinkage test (*note:* side surface refers to the surface with the dimensions of $280 \times 75\ mm^2$).

Fig. 3. Crack positions in circular and elliptical ring specimens.

cylinders and ring specimens. Their longitudinal length change was monitored by a dial gauge, which was then converted into shrinkage strain. Considering that concrete shrinkage depends on the A/V ratio of a concrete element, four different exposure conditions, i.e. representing four different A/V ratios, were investigated on concrete prisms in free shrinkage test. These include the scenarios of (1) all surfaces sealed, (2) all surface exposed, (3) two side surfaces sealed and (4) three side surfaces sealed, representing A/V ratio of 0, 0.0605, 0.0267, and 0.0133 mm^{-1}, respectively. It should be noted that side surface refers to the surface with the dimensions of 280×75 mm^2. In experiment, double-layer aluminum tape was used to seal the surfaces which were not intended for drying. Initial shrinkage measurement was carried out immediately after the concrete prisms were de-moulded at the age of 1 day and the measurements were continuously recorded twice per day until 28 days. Fig. 2 shows the measured free shrinkage strain of concrete at various ages under the four exposure conditions.

2.3. Restrained ring tests

As aforementioned, the restrained circular ring test has been widely used to assess cracking tendency of concrete and other cement-based materials. It has been found that cracking age depends on not only properties of concrete but also the degree of restraint provided by the central restraining steel core in the ring test [8,13]. In order to investigate the effects of geometry and shape of inner steel core on cracking of concrete surrounding it, both circular and elliptical concrete rings were prepared and subject to drying under restrained shrinkage till cracking initiated. The circular and elliptical rings tested in this study are illustrated in Fig. 1 with R_0 denoting the radius of the inner circumference of a circular concrete ring (see Fig. 1(a)) while R_1 and R_2 denoting the major and minor semi-axes, respectively, of the inner circumference of an elliptical concrete ring (see Fig. 1(b)).

According to the study of Zhou et al. [21], compared with traditional circular concrete rings, elliptical concrete rings with R_1/R_2 between 2 and 3 can provide higher degree of restraint leading to shorter cracking period in restrained shrinkage ring test so that to accelerate ring test. Therefore, in this study, for the concrete elliptical ring specimens with a 37.5 mm-thick wall same as that recommended by ASTM C1581/C1581M-09a, the inner major radius, R_1, was chosen as 150 mm and the inner minor radius, R_2, as 75 mm while the radius, R_0, of the inner circumference of the circular rings was designed as 150 mm same as R_1. In restrained ring test, four strain gauges were attached, each at one equidistant mid-height, on the inner cylindrical surface of the central restraining steel ring and they were connected to a data acquisition system in a half-bridge configuration which is able to automatically record the circumferential strain of the inner surface of the restraining steel ring continuously. Following ASTM C1581/C1581M-09a protocol, the top and bottom surfaces of the concrete ring specimens were sealed using two layers of aluminum tape and drying was only allowed through the outer circumferential cylindrical surface of the concrete rings. The strain gauges were then connected to the data acquisition system, and the instrumented ring specimens were finally moved into an environmental chamber for continuous drying under the temperature 23 °C and RH 50% till the first crack occurred. Cracking of concrete is indicated by the sudden drop in the measured strain, which is the same technique used for crack detection in restrained ring test recommended by both AASHTO PP34-99 and ASTM C1581/C1581M-09a. Two concrete ring specimens were tested per geometry. It was found that the cracking ages of the circular rings are 14 and 15 days, respectively, while those of the elliptical ones are both 10 days. Meanwhile, Fig. 3(a)–(c) present the crack positions of the circular and elliptical rings, respectively, obtained from experiment. It can be seen that, due to the effects of elliptical geometry, crack initiates close to the vertices on the major axis of an elliptical concrete ring as one may expect.

3. Numerical modelling

In this study, finite element analyses were carried out using ANSYS code to simulate stress development and calculate stress intensity factor in concrete ring specimens under restrained shrinkage. The numerical process can be divided into three steps, which are thermal, structural and fracture analyses. In thermal analysis, the 2-D 8-node thermal elements (PLANE77) were used for modelling concrete, which have compatible temperature shapes and are well suited to model

curved boundaries. Through thermal analysis, the temperature distribution in concrete can be achieved. In the following structural analysis, the elements for modelling concrete were replaced by the equivalent structural elements, i.e. PLANE183, which is a type of 2-D 8-node element with quadratic displacement behavior. PLANE183 elements are also well suited to modelling irregular meshes and support plasticity, creep, stress stiffening, large deflection and large strain. In order to eliminate the effect of friction between concrete and steel, the outer circumferential surface of the steel ring, which contacts the inner circumferential surface of the concrete ring, was coated with a release agent as suggested by ASTM C1581/C1581M-09a when preparing concrete ring tests. Accordingly, in numerical analyses, contact elements with zero friction between the contacting pairs were utilized to simulate this measure in conducting concrete ring tests in practice. The material parameters used in numerical analyses were as following: the elastic modulus and Poisson's ratio of steel both remain constant as 210 GPa and 0.3, respectively; the elastic modulus of concrete is determined using Eq. (1), which varies with age, and Poisson's ratio is set constant as 0.2. In fracture analysis, singular element was used to calculate SIF at crack tip. Because high stress gradients exist in the region around crack tip, special attention should be paid in that region. Therefore, a circle was set at the tip of crack, in which the crack tip is the center of the circle and the radius of the circle is 2 mm. The first row of elements around the crack tip had a radius of 1/2 mm, and their mid-side nodes were placed at the quarter points, i.e. had a radius of 1/8 mm.

3.1. Modelling of restrained shrinkage

Compared with a circular steel core, an elliptical one can provide higher degree of restraint to concrete surrounding it and also generate a non-uniform distribution of stress along its elliptical circumference when concrete is subject to drying shrinkage. The geometry factor R_1/R_2 of an elliptical ring dominates the degree of stress concentration in concrete and subsequently influences cracking age and position. Therefore, the conventional uniform internal pressure assumption widely adopted in analyzing restrained circular rings, which is used to simulate the effect of drying shrinkage, is not applicable to elliptical ones in restrained shrinkage test. In order to take into account the non-uniform stress distribution in elliptical concrete rings, a numerical approach was proposed to simulate the effect of geometry factor on cracking in concrete ring specimens subject to drying shrinkage. In this approach, a derived fictitious temperature field is applied to concrete to simulate the shrinkage effect so that a combined thermal and structural analysis can be adopted to analyze cracking in a concrete ring specimen caused by restrained shrinkage. With the implementation of the fictitious temperature field, shrinkage of concrete caused by the temperature field is restrained by the inner steel core, resulting in compressive stress developed in the steel core and tensile stress in the concrete ring. The derivation of the fictitious temperature field is elaborated elsewhere [21]. As the result of this exercise, Fig. 4 presents the derived relationship between fictitious temperature drop and A/V ratio at 3 days interval for a concrete element irrespective of its geometry/shape. For a given concrete ring with certain exposure condition (i.e. certain A/V ratio), the relationship between fictitious temperature drop and concrete age can be derived by linear interpolation from the relationship between A/V ratio and concrete age obtained in Fig. 4.

3.2. Crack driving energy rate curve (G-curve)

After the age-dependent fictitious temperature drop is determined, shrinkage effect can be simulated through applying the temperature drop on concrete in numerical analysis. When shrinkage of concrete is restrained by the inner steel ring, internal stress is developed in concrete, which is uniformly distributed in a circular ring but non-uniformly distributed in an elliptical ring. Fig. 5(a) and (b) present the restraining pressure on the inner circumferential concrete ring surface enforced by the central steel ring in a circular and an elliptical geometries, respectively, at the age of 10 days when concrete is subject to restrained shrinkage (in Fig. 5(a) and (b) the grey ring represents the concrete ring, circular or elliptical).

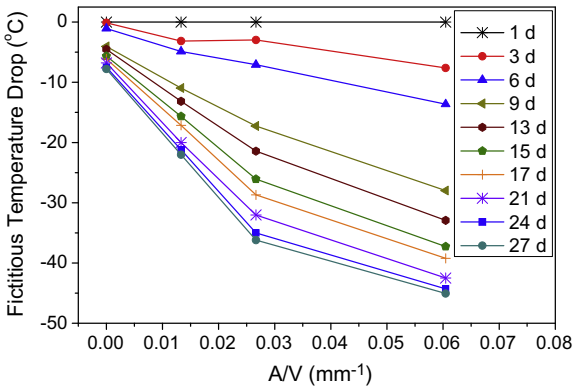

Fig. 4. Derived fictitious temperature drop with respect to A/V ratio for a concrete element.

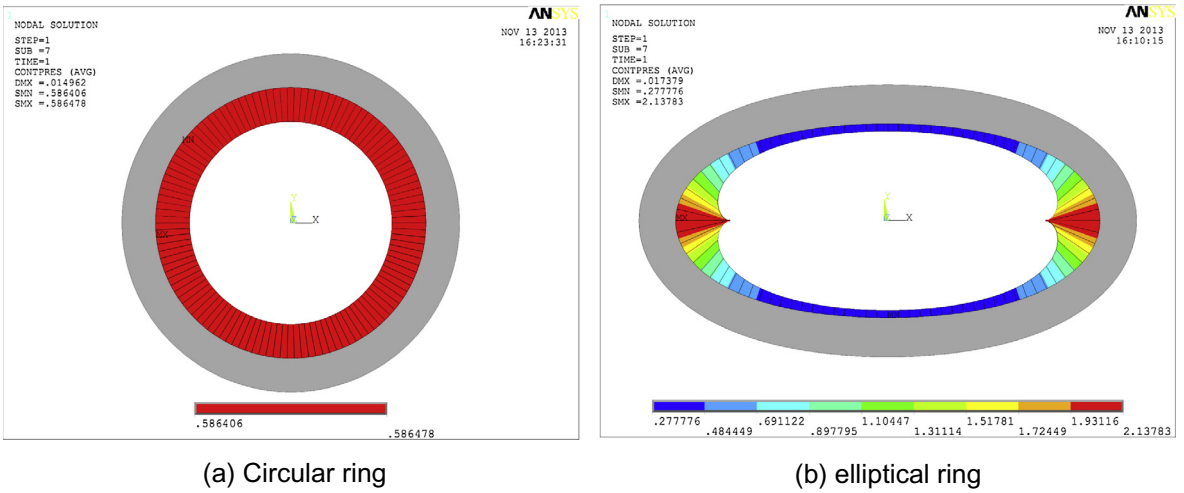

Fig. 5. Restraining pressure on the inner cylindrical concrete ring surface provided by the central steel ring.

It can be observed from this figure that the elliptical geometry dramatically influences the distribution of restraining pressure provided by the central steel ring when concrete is shrinking. At the same age, the pressure enforced on the circular concrete ring distributes uniformly along its inner circumference and the value is 0.59 MPa; while the pressure on the elliptical one distributes non-uniformly, with the maximum and minimum values being 2.14 MPa and 0.28 MPa, and occurring on the vertices of the major and minor axes, respectively. It can be seen that the maximum restraining pressure increases from 0.59 MPa on the circular ring to 2.14 MPa on the elliptical ring, the latter being 3.6 times of the former. Therefore, it can be concluded that the enhancement of restraining effect is significant by using elliptical geometry in restrained shrinkage test.

In this study, finite element method was used to calculate the stress intensity factor (K_I) for the circular and elliptical rings. Based on the classic fracture mechanics theory, K_I can be defined as following

$$K_I = \sigma\sqrt{\pi a f}(a/w) \tag{5}$$

where a is the crack length, σ is the nominal stress which represents the circumferential tensile stress at the inner circumference of a ring specimen, w is the concrete ring wall thickness, i.e. 37.5 mm in this study, and $f(a/w)$ is a geometrical function. It has been found that, in case of thin concrete rings with a ring wall thickness of 37.5 mm, crack initiates on the inner circumferential surface when subject to restrained shrinkage [21]. Particularly, in the case of an elliptical ring, crack initiates on the vertices of its major axis. Thus, in the fracture analyses conducted in this study, the pre-cracks in the circular and the elliptical concrete rings are set as shown in Fig. 6. In numerical analysis, the pressure extracted from Fig. 5 is applied on the inner circumferential surface of a concrete ring with a pre-crack (see Fig. 6). With a pre-crack, a fracture mechanics-based analysis can thus be performed.

After the fictitious temperature drops are derived for the circular/elliptical ring at various ages, they are applied on the restrained concrete ring in a combined thermal and fracture analysis to simulate the mechanical effect of shrinkage of

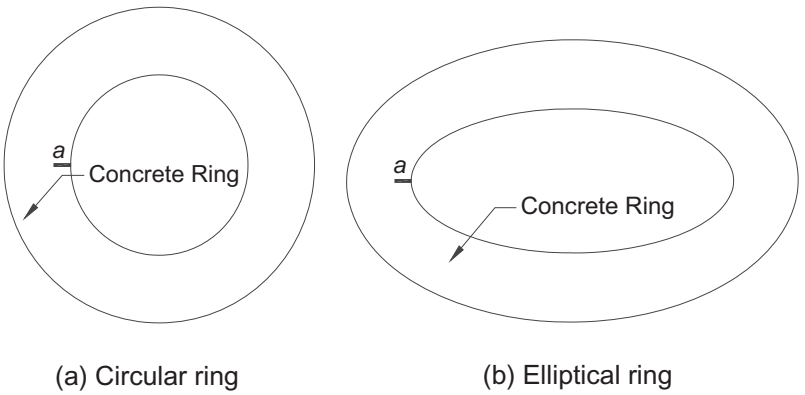

Fig. 6. Pre-crack in concrete ring specimens.

concrete. It is generally regarded that moisture gradient across a concrete section can influence shrinkage of concrete. The assumption of uniform shrinkage across a concrete ring wall is acceptable when the influence of moisture gradient is less significant [9,13], for example, in the case of a concrete ring specimen drying from its top and bottom surfaces in restrained shrinkage test. Based on this assumption, crack initiates at the inner circumferential surface and propagates towards the outer one of a restrained concrete ring specimen. When the influence of moisture gradient becomes significant, the non-uniform shrinkage across a concrete ring wall leads to higher tensile stress at the outer circumference than at the inner one of a restrained concrete ring. This subsequently results in crack initiating at the outer circumference [13], for instance, in the scenario that the ring specimens with a 75 mm thick wall drying from the outer circumference in restrained shrinkage test. However, comparing with the scenario of a thick concrete ring specimen with a 75 mm thick wall, the influence of moisture gradient on shrinkage of concrete is not significant in the case of a thin concrete ring specimen with the wall thickness of 37.5 mm. In line with this, it is approximately assumed in this study that shrinkage of concrete is uniform across the wall of a 37.5 mm-thick concrete ring specimen. On the other hand, it was found that crack initiated at the inner circumferential surface in all thin ring specimens tested in this study, which verifies the uniform shrinkage assumption. Accordingly, in this study the fictitious temperature field, simulating the effect of concrete shrinkage, was reasonably assumed uniform across the wall of the thin concrete ring specimens with a 37.5 mm thick wall.

According to Eq. (5), the stress intensity factors for circular and elliptical rings under restrained condition can be derived based on the stress state and geometry function at any given crack length. By applying the fictitious temperature field on a restrained concrete ring specimen, the restraining pressure on concrete enforced by a central steel ring can be derived through numerical analysis, which is further represented by loading acting on the concrete ring with an initial crack for fracture analysis. Since the equivalent loading is determined based on the fictitious temperature field, the stress state in concrete is related to elastic modulus, fictitious temperature field simulating the mechanical effect of shrinkage, and linear thermal expansion coefficient of concrete. Meanwhile, the geometry functions of circular and elliptical rings can be derived through numerical analyses based on the ring geometry. The pre-cracks in the circular and the elliptical concrete rings are set as shown in Fig. 6. Through varying the initial crack length from 2 to 32 mm with 2 mm interval, the stress intensity factor at the tip of initial crack can be calculated numerically based on displacement extrapolation method using ANSYS code. Further, the coefficients of geometry function and stress states at various ages can be obtained through regression analyses which results in continuous equations, i.e. Eqs. (6) and (7), of stress intensity factor for circular and elliptical rings, respectively. Fig. 7 illustrates the finite element meshes of concrete rings with an initial crack length a = 12 mm, in which Fig. 7(a) and (b) present the overall mesh in a circular and an elliptical ring, respectively, and Fig. 7(c) shows the refined mesh at crack tip. According to the numerical analysis results obtained using finite element method, the stress intensity factor K_I in MPa mm$^{1/2}$ of the circular ring with the geometry and pre-crack shown in Fig. 7(a) can be formulated as

$$K_I = -4.41 \times 10^3 T \cdot E \cdot \alpha_c \sqrt{\pi a}(2.12 + 1.26(a/w) - 0.71(a/w)^2 + 14.22(a/w)^3 - 10.05(a/w)^4) \quad (6)$$

While that of the elliptical ring with the geometry and pre-crack depicted in Fig. 7(b) can be expressed as

$$K_I = -21.76 \times 10^3 T \cdot E \cdot \alpha_c \sqrt{\pi a}(0.68 - 0.8(a/w) + 2.93(a/w)^2 - 1.73(a/w)^3 + 0.2(a/w)^4) \quad (7)$$

In which T (in °C) is the fictitious temperature drop acting on a concrete ring representing the effect of drying shrinkage, E is the elastic modulus of concrete (in GPa), and α_c is the linear thermal expansion coefficient of concrete (in 1/°C). Based on classical fracture mechanics theory, the energy supplied for crack propagation, i.e. G-curve, can be derived based on K_I and modulus of elasticity of material E as following:

$$G = K_I^2 / E \quad (8)$$

Fig. 8 illustrates the derived G-curves of both the circular and the elliptical rings at the ages of 5, 10, 15, 20 days, respectively. It can be seen that, even with the same geometry, the G-curves increase with the increase of concrete age. It is worth pointing out here that, at a given concrete age, the circular and elliptical rings demonstrate different features with the increase of crack length a. When a < 24 mm, the crack driving energy rate in the elliptical ring is greater than that in the

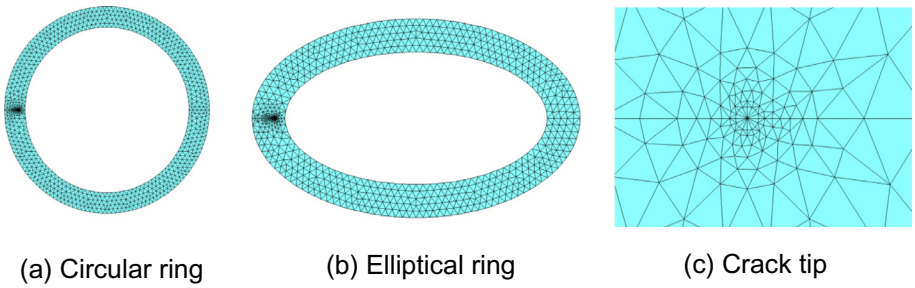

Fig. 7. Finite element meshes of concrete rings and at crack tip.

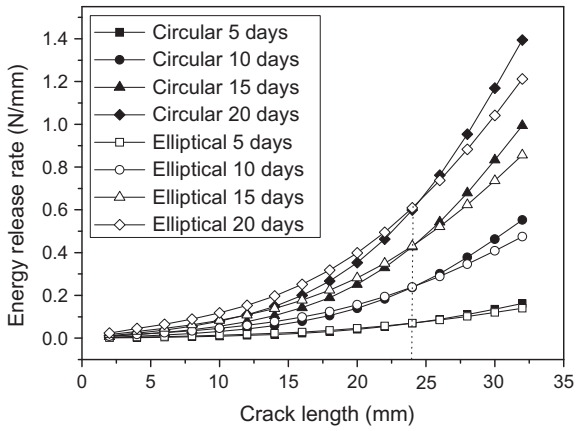

Fig. 8. *G*-curves of circular and elliptical rings at various ages.

circular ring, indicating that the elliptical ring may crack earlier than the circular one if the critical crack length is less than 24 mm. However, when $a > 24$ mm, the crack driving energy rate in the circular ring is greater than that in the elliptical ring, suggesting that the circular ring may crack earlier than the elliptical one if the critical crack length is greater than 24 mm.

3.3. Resistance curve (R-Curve)

The resistance curve (*R*-Curve) method presented here is based on the work of Ouyang and Shah [25] and Shah et al. [19] for investigating crack propagation in concrete. The *R*-curve is formulated as

$$R = \beta\psi(a - a_0)^{d_2} \tag{9}$$

$$d_{1,2} = \frac{1}{2} + \frac{\alpha - 1}{\alpha} \pm \left[\frac{1}{4} + \frac{\alpha - 1}{\alpha} - \left(\frac{\alpha - 1}{\alpha}\right)^2\right]^{\frac{1}{2}} \tag{10}$$

$$\psi = 1 - \frac{(d_2\alpha - \alpha + 1)}{(d_1\alpha - \alpha + 1)}\left(\frac{\alpha a_0 - a_0}{a - a_0}\right)^{d_2 - d_1} \tag{11}$$

where $\alpha = a_c/a_0$, a_c is the critical crack length and a_0 is the initial crack length. In order to obtain reasonable results for an uncracked concrete specimen, like the circular or elliptical concrete rings investigated in this study through fracture analyses, the initial crack length should remain reasonably as small as possible by considering the sizes of aggregates. In the research of Ouyang and Shah [25], initial crack length was chosen as 2 mm for concrete elements. As long as this value remains reasonably small, it has been found that the overall fracture analysis results on the same concrete elements but with different initial crack lengths are very close by using the *R*-curve method. Therefore, in order to reduce the effects of arbitrariness of a_0 on fracture analysis results of an actually un-cracked concrete ring specimen, a_0 should be reasonably as small as possible, which was chosen as 2 mm in this study for both the circular and the elliptical concrete rings. Moreover, for the determination of parameters α and β, Shah et al. [19] developed an expression (see Eq. (12)) based on an infinitely large plate with a single edge-notch (SEN) pre-crack under tensile loading as following. Firstly, stress intensity factor (K_{IC}) and critical crack tip opening displacement ($CTOD_c$) can be derived numerically. Then, an expression can be obtained by substituting $CTOD_c$ into K_{IC}, which is presented as following

$$\frac{0.117 CTOD_c^2 E^2}{(K_{IC})^2 a_0} = \alpha\left(1 - \frac{1}{\alpha^2}\right)\left[1 - \frac{0.5}{\alpha} + \frac{0.434}{\alpha^2} - \frac{0.154}{\alpha^3}\right]^2 \tag{12}$$

Once $CTOD_c$ and K_{IC}, which are two fracture parameters of concrete, are derived from three-point bending test results of notched beams conforming to the recommendation of RILEM on TPFM, α can be determined using Eq. (12). Further, β is obtained by satisfying the equation of $R = K_I^2/E$, which can be expressed as

$$\beta = \frac{(K_{IC})^2(\alpha a_0 - a_0)^{-d_2}}{E\left(1 - \frac{d_2\alpha - \alpha + 1}{d_1\alpha - \alpha + 1}\right)} \tag{13}$$

It should be noted that the *R*-curve derived from Eqs. (9)–(13) is based on the geometry of an infinitely large plate. However, according to Ouyang and Shah [25], for the same geometry and initial crack length, the derived *R*-curve also applies to finite size specimens. *R*-curve is defined as an envelope of *G*-curves with different specimen sizes but the same initial crack

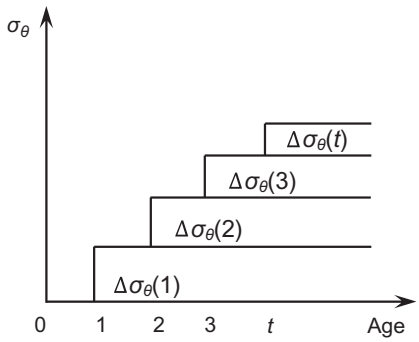

Fig. 9. Illustration of creep estimation in numerical analysis.

length [25]. Weiss et al. [8] have verified that the R-curves for circular ring specimens with different characteristic sizes but the same initial crack length are similar to that of an infinitely large plate. Therefore, in this study the R-curves for the circular and elliptical rings were approximately taken as that of an infinite large plate with a SEN pre-crack.

3.4. Creep

Since the derivation of fictitious temperature drop is based on volume change of concrete prisms subject to free shrinkage test, the effect of creep on strain in a ring specimen is not taken into account when using the fictitious temperature drop to

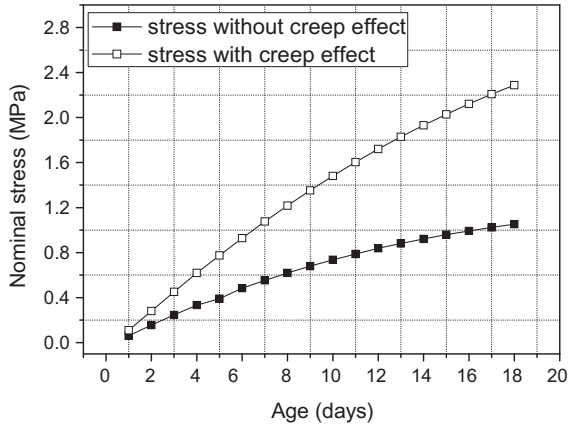

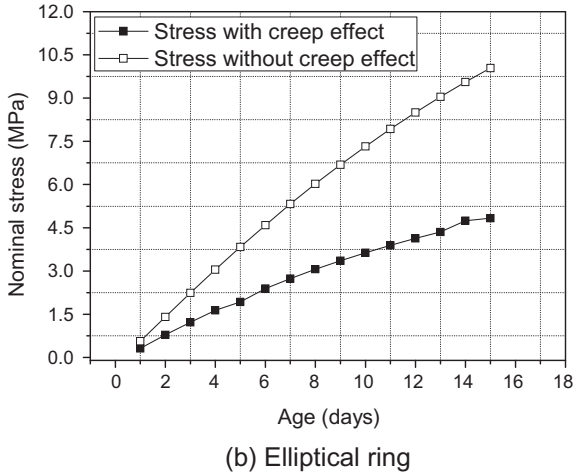

Fig. 10. Nominal stress in restrained concrete rings with and without consideration of concrete creep effect.

simulate the shrinkage effect of concrete. But actually cracking of a concrete ring specimen is affected by not only shrinkage but also creep, two unique material properties of concrete which not many other engineering materials possess one or both of them. Therefore, it is significant to estimate the magnitude of creep during the process of restrained shrinkage in concrete. In this study creep of concrete is estimated using the formula recommended by CEB-FIP Model Code 2010, in which the total strain is the sum of elastic strain and creep strain and can be expressed as

$$\varepsilon_{c\sigma}(t,t_0)=\sigma_c(t_0)\left[\frac{1}{E_{ci}(t_0)}+\frac{\varphi(t,t_0)}{E_{ci}}\right]=\sigma_c(t_0)J(t,t_0) \tag{14}$$

where $\varepsilon_{c\sigma}(t,t_0)$ is the stress-dependent strain of concrete at time t, $\sigma_c(t_0)$ is the stress in concrete at the time of loading t_0, $E_{ci}(t_0)$ is the modulus of elasticity of concrete at the time of loading t_0, E_{ci} is the modulus of elasticity of concrete at the age of 28 days, $J(t,t_0)$ is the creep function, and $\varphi(t,t_0)$ is the creep coefficient. Details for obtaining these parameters can be referenced to CEB-FIP Model Code 2010. Since $\varepsilon_{c\sigma}(t,t_0)$ depends on the circumferential tensile stress of a concrete ring under restrained shrinkage, the stress can be divided into many increments $\Delta\sigma_\theta$, which is caused by shrinkage of concrete increasing with age. For example, when investigating the effects of creep at 10th day, the stress increment $\Delta\sigma_\theta(1)$ caused by shrinkage at the first day will affect that at the following 10 days, and the stress increment $\Delta\sigma_\theta(2)$ caused by shrinkage at the second day will only affect that of the following 9 days. This process is schematically illustrated in Fig. 9. After taking into account the creep effect of concrete, the nominal stress in the circular and elliptical rings was calculated and presented in Fig. 10(a) and (b), respectively. The nominal stress, without the consideration of concrete creep, in the circular and elliptical rings was also presented for comparison purpose in Fig. 10. It can be seen that, with the consideration of creep, the nominal stress in both circular and elliptical concrete rings become much smaller as expected.

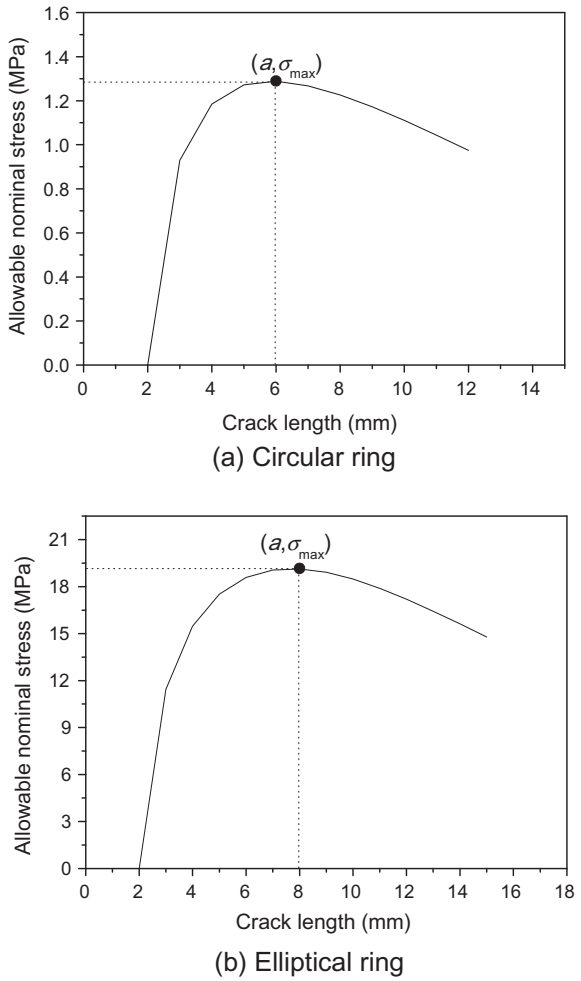

Fig. 11. Allowable nominal stress in concrete rings from fracture analysis.

3.5. Cracking age

In the restrained shrinkage ring test, cracking age of a concrete ring is determined by the abrupt drop observed from the measured steel strain, which is the same technique adopted by AASHTO PP34-99 and ASTM C1581/C1581M-09a in determining cracking age of concrete in restrained ring test [21]. If the restraining effect provided by the steel ring can be regarded as the externally applied load on concrete in a fracture analysis of ring specimens, the abrupt strain drop indicates that the applied load has reached its peak. Correspondingly, the crack in concrete has evolved from stable to unstable propagation stage with a critical crack length a_c. Then, at the critical state corresponding to $a = a_c$, the G- and R-curves intersect and have the same slope, i.e. mathematically

$$G = R = (K_{IC})^2/E \tag{15}$$

and

$$\frac{\partial G}{\partial a} = \frac{\partial R}{\partial a} \tag{16}$$

After that moment, concrete enters the unstable propagation stage corresponding to $a > a_c$. R-curve should keep a plateau with the value of $(K_{IC})^2/E$. It should be noted that, due to the effect of specimen size, the critical crack length for a finite-size specimen is a_c^f rather than a_c obtained from an infinite-size specimen. By substituting Eqs. (8) and (9) into Eqs. (15) and (16), two nonlinear equations are resulted yielding the two unknown parameters a_c^f and the corresponding critical nominal stress σ_c. Further, the critical fictitious temperature drop at the critical nominal stress σ_c can be determined. Through comparing the critical fictitious temperature drop obtained from fracture analysis with the age-dependent one derived from free shrinkage test, the cracking age can be determined.

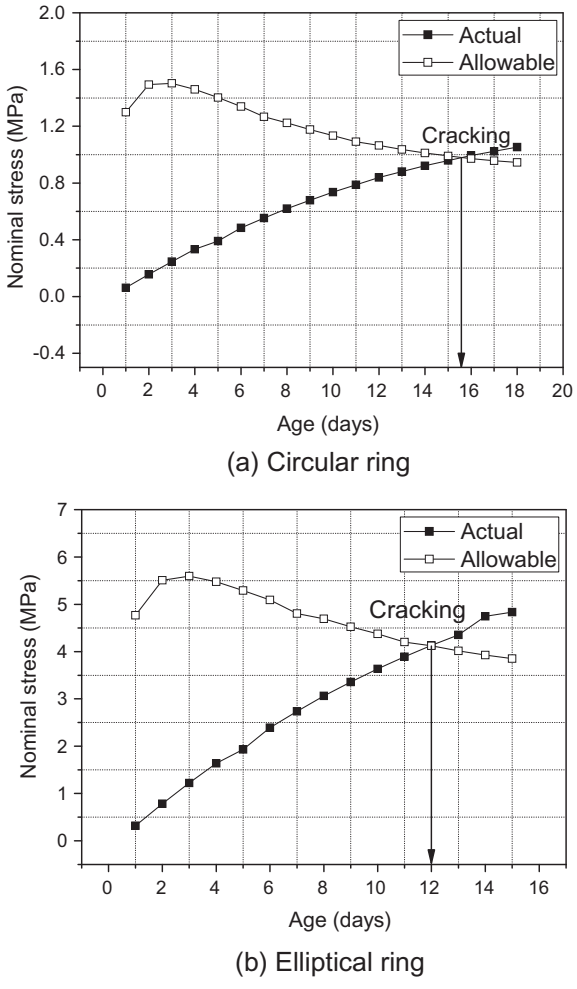

Fig. 12. Schematic illustration of determination of cracking age for concrete rings.

Table 1
Cracking ages (in days) of concrete rings from experiment and fracture analysis.

Circular ring			Elliptical ring		
Experiment		Prediction	Experiment		Prediction
14	15	16	10	10	12

Alternatively, cracking age of a restrained concrete ring can be determined by maximizing nominal stress σ and comparing it with the maximum allowable tensile stress. This alternative method is actually adopted in this study for determining cracking age of both circular and elliptical concrete rings under restrained shrinkage. According to the condition of $G = R$, the relationship between crack length a and allowable nominal stress σ can be determined. Fig. 11(a) and (b) illustrate such relationships for the circular and elliptical rings at the age of 10 days, respectively. It can be seen clearly that there is a peak value for the allowable nominal stress, i.e., σ_{max} in the figures. Because this value is obtained from R-curve, it indicates the maximum resistance of a concrete ring at a given age. Collecting σ_{max} for each day, the relationship between allowable nominal tensile stress and concrete age can be established, which is presented in Fig. 12. At the same time, when the actual nominal stress, which is caused by fictitious temperature drop simulating the mechanical effect of shrinkage and with the consideration of creep, exceeds the maximum allowable nominal stress, the ring specimen cracks. The corresponding crack length is the critical crack length a_c^f for the ring specimen. It can be seen from the results shown in Fig. 12 that the cracking age of the circular ring is approximately 16 days and that of the elliptical one is approximately 12 days. These values are compared with their counterparts from experiment (see Table 1). It can be seen that they agree reasonably well with their experimental counterparts, indicating that the fracture analysis model proposed in this study for predicting crack initiation in concrete ring specimens subject to restrained shrinkage is reliable. Compared with traditional circular rings, elliptical ring with $a/b = 2$ can provide higher degree of restraint which leads to shorter cracking period in restrained shrinkage ring test.

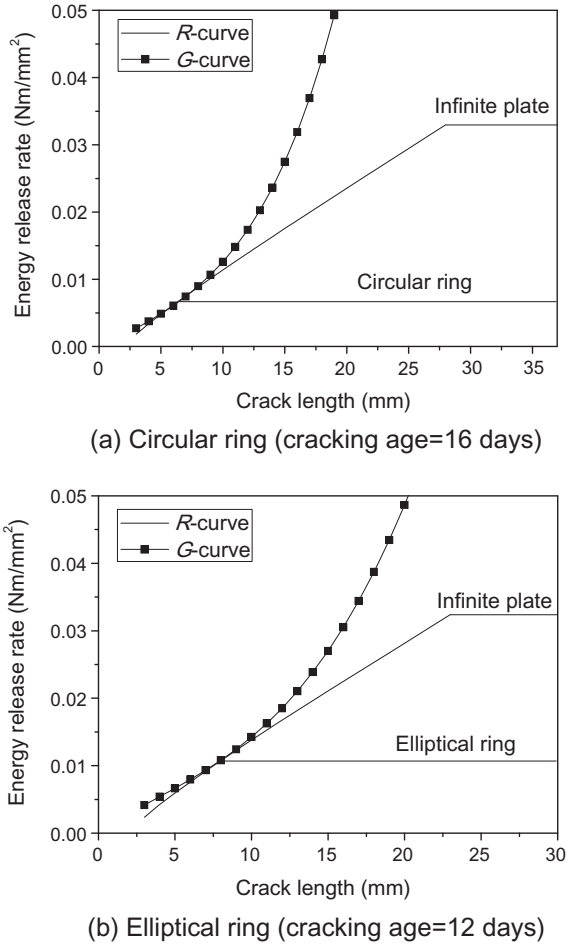

Fig. 13. G- and R-curves obtained from the fracture analysis.

Based on the cracking age derived from Fig. 12, the *G*- and *R*-curves for circular and elliptical rings are illustrated in Fig. 13(a) and (b), respectively. At the cracking ages, *G*- and *R*-curves intersect and also have the same slope. The crack length corresponding to the point of intersection is the critical crack length a_c^f for a ring specimen. After this point, the *R*-curve reaches a plateau while *G*-curve keeps increasing overwhelming the *R*-curve, indicating fracture failure of the ring specimen.

4. Conclusions

A numerical approach based on fracture mechanics has been developed for predicting concrete cracking in restrained circular and elliptical ring specimens subject to drying shrinkage. Ring specimens are widely used for assessing cracking tendency of concrete and other cement-based materials with the circular ring test has become a standard method recommended by both AASHTO and ASTM. The derived fictitious temperature field was used to simulate the effect of shrinkage in circular and elliptical ring specimens. The driving energy for crack propagation in a ring specimen can be determined numerically while the resistance to crack propagation can also be derived based on measured fracture parameters of concrete. Cracking age of restrained concrete rings can be determined by comparing the *G*- and *R*-curves. The following conclusions can be drawn:

(a) Cracking ages from numerical analyses agreed well with experimental results for circular and elliptical ring specimens. It indicates that using a fictitious temperature field to simulate the shrinkage of concrete and introducing resistance curve to investigate the cracking behavior of concrete in restrained shrinkage test are appropriate and reliable.
(b) Based on experimental and numerical results, it can be seen that the elliptical ring with $R_1/R_2 = 2$ cracks earlier than the circular ring, which can shorten the cracking period in restrained shrinkage ring test. The numerical results indicate that restraining pressure caused by shrinkage enforced on a circular concrete ring distributes uniformly along its circumference, while that on an elliptical one distributes non-uniformly. Due to geometry effect, the maximum circumferential tensile stress in an elliptical ring is about 3.6 times of that in a circular ring, which promotes markedly the restraint effect on concrete in restrained shrinkage test.
(c) According to the evolution of crack driving energy rate, in addition to the geometry effect, it is the critical crack length a_c^f corresponding to unstable cracking propagation which determines the advantage of using elliptical geometry in restrained ring test to shorten test duration. For the normal strength concrete investigated in this research, when $a_c^f < 24$ mm, the driving energy in an elliptical ring is greater than that in a circular ring indicating that elliptical geometry can provide higher degree of restraint. In contrast, when $a_c^f > 24$ mm, things are different. The driving energy in an elliptical ring becomes less than that in a circular ring, indicating that an elliptical ring needs a longer period to crack.

Acknowledgments

The financial support of the UK Engineering and Physical Sciences Research Council under the grant of EP/I031952/1, and the National Natural Science Foundation of China under the grant of NSFC 51121005/51109026 is gratefully acknowledged.

References

[1] Parilee AM, Buil M, Serrano JJ. Effect of fiber addition on the autogenous shrinkage of silica fume concrete. ACI Mater J 1989;86(2):139–44.
[2] Kovler K. Testing system for determining the mechanical behavior of early age concrete under restrained and free uniaxial shrinkage. RILEM Mater Struct 1994;27(6):324–30.
[3] Kraai PP. A proposed test to determine the cracking potential due to drying shrinkage of concrete. Concr Construct 1985;30(9):775–8.
[4] Shales CA, Hover KC. Influence of mix-proportion and construction operations on plastic shrinkage cracking in thin slabs. ACI Mater J 1988;85(6):495–504.
[5] Carlson RC, Reading TJ. Model of studying shrinkage cracking in concrete building wall. ACI Struct J 1998;85(4):395–404.
[6] Grzybowski M, Shah SP. Shrinkage cracking of fiber reinforced concrete. ACI Mater J 1990;87(2):138–48.
[7] Weiss WJ. Prediction of early-age shrinkage cracking in concrete. Ph.D Dissertation, Northwestern University, Evanston, Illinois; 1999.
[8] Weiss WJ, Yang W, Shah SP. Influence of specimen size/geometry on shrinkage cracking of rings. ASCE J Engng Mech 2000;126(1):93–101.
[9] Weiss WJ, Shah SP. Restrained shrinkage cracking: the role of shrinkage reducing admixtures and specimen geometry. RILEM Mater Struct 2002;35(3):85–91.
[10] Bentur A, Kovler K. Evaluation of early age cracking characteristics in cementitious systems. RILEM Mater Struct 2003;36(3):183–90.
[11] Moon JH, Pease B, Weiss J. Quantifying the influence of specimen geometry on the results of the restrained ring test. J ASTM Int 2006;3(8):1–14.
[12] Hossain AB, Weiss J. Assessing residual stress development and stress relaxation in restrained concrete ring specimens. Cem Concr Comp 2004;26(5):531–40.
[13] Hossain AB, Weiss J. The role of specimen geometry and boundary conditions on stress development and cracking in the restrained ring test. Cem Concr Res 2006;36(1):189–99.
[14] Moon JH, Weiss J. Estimating residual stress in the restrained ring test under circumferential drying. Cem Concr Comp 2006;28(5):486–96.
[15] Passuello A, Moriconi G, Shah SP. Cracking behavior of concrete with shrinkage reducing admixtures and PVA fibers. Cem Concr Comp 2009;31(10):699–704.
[16] He Z, Zhou XM, Li ZJ. New experimental method for studying early-age cracking of cement-based materials. ACI Mater J 2004;101(1):50–6.
[17] He Z, Li ZJ. Influence of alkali on restrained shrinkage behavior of cement-based materials. Cem Concr Res 2005;35(3):457–63.
[18] He Z, Li ZJ, Chen MZ, Liang WQ. Properties of shrinkage-reducing admixture-modified pastes and mortar. RILEM Mater Struct 2006;39(4):445–53.
[19] Shah SP, Ouyang C, Marikunte S, Yang W, Becq-Giraudon EA. A method to predict shrinkage cracking of concrete. ACI Mater J 1998;95(4):339–46.
[20] Shah HR, Weiss WJ. Quantifying shrinkage cracking in fiber reinforced concrete using the ring test. RILEM Mater Struct 2006;39(9):887–99.

[21] Zhou XM, Dong W, Oladiran O. Assessment of restrained shrinkage cracking of concrete using elliptical ring specimens: experimental and numerical. ASCE J Mater Civ Engng 2014. http://dx.doi.org/10.1061/(ASCE) MT. 1943-5533.000100.
[22] Turcry P, Loukili A, Haidar K, Pijaudier CG, Belarbi A. Cracking tendency of self-compacting concrete subjected to restrained shrinkage: experimental study and modeling. J Mater Civ Engng 2006;18(1):46–54.
[23] Wu XR, Carlson AJ. Weight function and stress intensity factors. Pergamon, Tarrytown, N.J; 1990.
[24] Shah SP. RILEM committee on fracture mechanics of concrete-test methods, determination of the fracture parameters (K_{Ic}^{s} and $CTOD_c$) of plain concrete using three-point bend tests. RILEM Mater Struct 1990;23(6):457–60.
[25] Ouyang CS, Shah SP. Geometry-dependent R-curve for quasi-brittle materials. J Am Ceram Soc 1991;74(11):2831–6.